JOURNAL OF MATERIALS SCIENCE **37** (2002) 5333–5337

A study on gradient thermal barrier coatings by EB-PVD in a cyclic high-temperature hot-corrosion environment

HONGBO GUO, HUIBIN XU, SHENGKAI GONG
School of Materials Science and Engineering, Beijing University of Aeronautics and Astronautics, Beijing, 100083, People's Republic of China
E-mail: guohobo@263.net

Gradient thermal barrier coatings (GTBCs) have been produced by electron beam physical vapor deposition (EB-PVD). Their performance was evaluated by isothermal oxidation and cyclic high-temperature hot-corrosion tests. It is found that the GTBCs exhibited better resistance to high-temperature oxidation and cyclic high-temperature hot-corrosion (HTHC) than traditional two-layered TBCs. A dense Al_2O_3 layer on the bond coat of GTBCs can effectively prohibit inward diffusion of oxidants such as O and S and outward diffusion of Al and Cr. On the other hand, an "inlaid" interface, the formation of which resulted from the oxidation of Al diffusion into the gaps between the columns of bond coat during the fabrication of the GTBCs, contributes to reinforce the adherence of the Al_2O_3 layer to the bond coat. During fluxing of the Al_2O_3 layer, S and O diffused into the bond coat. Cracks developed in the surface layer of bond coat by the combined effect of sulfidation of the bond coat and thermal cycling, and finally led to failure of the GTBC.

1. Introduction

Thermal barrier coatings (TBCs) have exhibited an increasing potential in improving the durability and efficiency of gas turbine engines by allowing an increase in turbine inlet temperature (TIT), and by reducing the amount of cooling air required by hot-section components [1]. TBCs produced by electron beam physical vapor deposition (EB-PVD) have shown considerable improvement in tolerance to thermal cycling as compared with those by plasma spraying (PS) [2–5]. The superior performance of EB-PVD coatings has been attributed to development of a columnar microstructure. Recently, gradient thermal barrier coatings (GTBCs) are produced by co-deposition of a tablet of mixtures of Al-Al_2O_3-YSZ onto NiCoCrAlY bond coat by means of EB-PVD [6, 7]. Relative to traditional two-layered coatings, the GTBCs have the advantages of forming continuous microstructure through the thickness of the coating and consequently avoiding stress concentration in the coating.

As one of crucial problems unavoidable met in application, hot corrosion behavior is an important aspect of research on properties of TBCs. Some investigation has been performed on possible effects of hot-corrosion attack on the traditional two-layered coatings initially by [8] and latter by Jones *et al.* [9] and James *et al.* [10]. Compared with those tested in oxidation environment, the lifetimes of the two-layered coatings drop precipitously when tested in hot-corrosion environment [11]. Several mechanisms have been proposed to explain the accelerated degradation of the TBCs in the hot-corrosion conditions: destabilization of zirconia, accelerated oxidation and sulfidation of bond coat, solidification of sodium sulphate in cracks [12]. However, no investigation so far has been made on failure mechanism of the GTBCs under hot-corrosion. In the present study, an effort was made to evaluate performance of the GTBCs by isothermal oxidation and cyclic high-temperature hot-corrosion (HTHC) tests.

2. Experimental

2.1. Preparation of GTBCs

A four-electron-gun EB-PVD equipment with three water-cooled copper crucibles were used for preparing the GTBCs. A Ni-based superalloy was chosen to be the substrate material. The specimens were dimensioned as 15 mm × 10 mm × 2 mm. NiCoCrAlY and ZrO_2-8wt%Y_2O_3 (YSZ) ingots of 50 mm in diameter and 200 mm in length were used as the evaporation sources of the bond coat and the ceramic topcoat, respectively. The chemical composition of the NiCoCrAlY ingot was Ni-22Co-20Cr-8Al-1Y in wt%. A tablet pressed from mixtures of powders of Al-Al_2O_3-ZrO_2-8wt%Y_2O_3 was placed on the upper end face of the YSZ ingot to act as the evaporation source of a transition layer between the bond coat and YSZ topcoat. A NiCoCrAlY bond coat was first deposited onto the substrate by EB-PVD. Then, the tablet of Al-Al_2O_3-ZrO_2-8wt%Y_2O_3 was co-deposited onto the bond coat also by EB-PVD. And finally, the GTBCs were finished by the deposition of an

YSZ topcoat. Detailed procedures about the fabrication of the GTBCs were already been given elsewhere [6]. As the result, a GTBC can be obtained with the structure of NiCoCrAlY bond coat/Al_2O_3 layer/Al_2O_3-YSZ transition layer/YSZ topcoat.

For comparison, traditional two-layered TBCs comprising of NiCoCrAlY bond coat and YSZ topcoat were also prepared by means of EB-PVD, where the bond coat was pre-oxidized in vacuum and surface-strengthened by shot-peening before deposition of YSZ topcoat onto the bond coat. The thickness of the bond coat and YSZ topcoat of the two-layered coating are the same as those of the GTBCs, respectively.

2.2. Isothermal oxidation tests

Isothermal oxidation tests were performed using a thermal analytical balance of TG 328A model. The test specimens were exposure to air at 1323 K for 100 hr and their weight changes were measured to a precision of 10^{-4}g.

2.3. High-temperature-corrosion tests [13, 14]

The HTHC is generally defined as hot corrosion that occurs at temperature above the melting point of Na_2SO_4 ($>$1157 K). The tested specimens were weighed by the thermal analytical balance and coated with a 2 mg/cm^2 deposit of Na_2SO_4 sprayed onto all sides of the test specimens (preheated to 373 K) with an aqueous solution of Na_2SO_4. The test specimens were inserted the air furnace at 1223 K and removed after 20 hr. Subsequently, the specimens were cooled to room temperature and rinsed several times with deionized water and furnace dried, recoated with Na_2SO_4, reweighed and reinserted the furnace.

3. Results and discussion

3.1. GTBCs before testing

Fig. 1 shows an SEM micrograph and EDXS mappings of cross-section of the GTBC before testing. The GTBC consists of a NiCoCrAlY bond coat (about 50 μm), an Al_2O_3 layer (about 5 μm), an Al_2O_3-YSZ transition layer (about 10 μm) and an YSZ topcoat (about 80 μm). The Al_2O_3 layer was formed during the deposition of the tablet of Al-Al_2O_3-YSZ onto the bond coat. It is well known that for traditional two-layered TBCs a fully dense TGO can not obtained under thermal cycling, due to mismatch of coefficient of thermal expansion (CTE) [15–17]. It can be speculated that the GTBCs have a better resistance to oxidation than tradition two-layered TBCs.

3.2. Isothermal oxidation tests

Isothermal-oxidation tests were performed to understand the growth mechanism of oxides in the GTBC. For comparison, specimens with the two-layered TBC, and with the single NiCoCrAlY coating were also used for the tests. Fig. 2 shows the weight changes of the coated specimens during 100 hr testing in air at 1323 K. The oxidation reactions generally followed the parabolic rate law. The weight gains after 100 hr testing were 0.38 mg/cm^2, 0.45 mg/cm^2 and 0.72 mg/cm^2 for the GTBC, the two-layer TBC and the single NiCoCrAlY coating, respectively. According to the parabolic rate law $m^2 = k_\text{p}t$ (where m is specific weight gain, k_p is parabolic rate constant, and t is time)

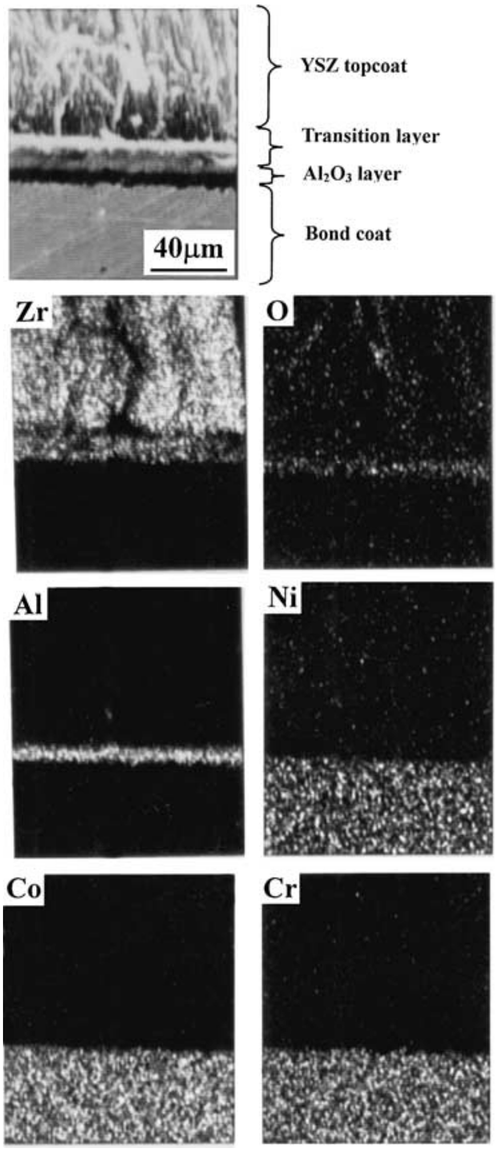

Figure 1 SEM micrograph and EDXS analysis of cross-section of the GTBC before testing.

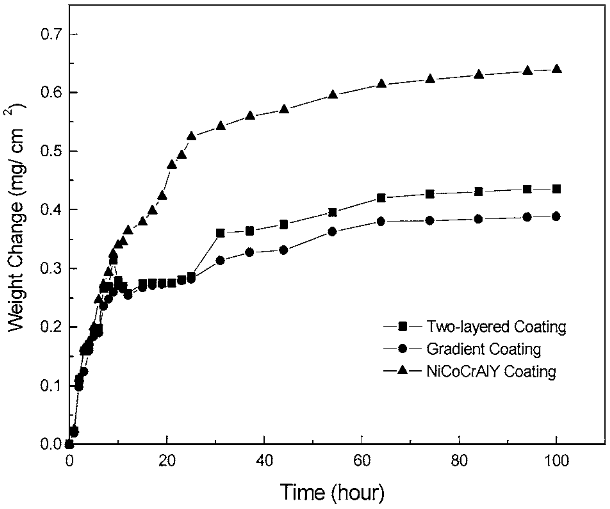

Figure 2 Plot of weight change vs. time for the coated specimens during 100 hr testing in air at 1050°C.

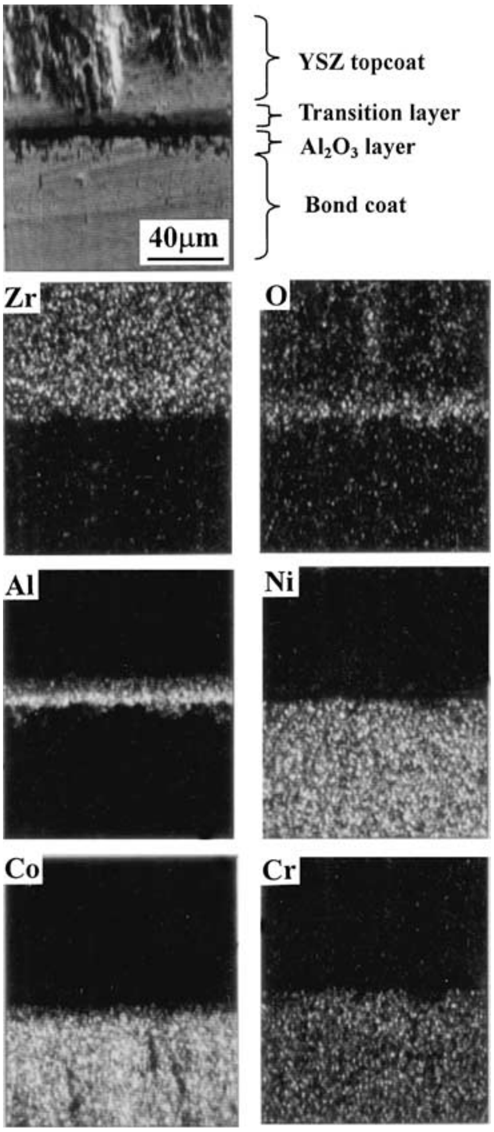

Figure 3 SEM micrograph and EDXS analysis of cross-section of the GTBC after 100 hr testing in air at 1323 K.

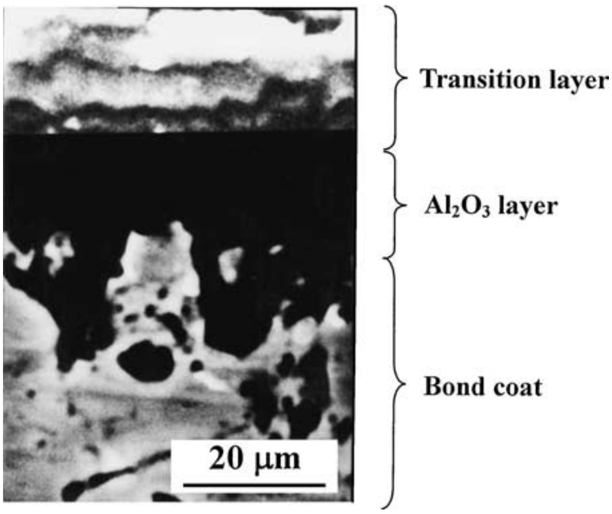

Figure 4 Higher magnification of the "inlaid" interface between the Al_2O_3 layer and bond coat in Fig. 3, where the Al_2O_3 layer grew into gaps between the columnar grains in the bond coat.

[18], the oxidation rate constants were calculated to be 4.011×10^{-13} $g^2cm^{-4}s^{-1}$, 5.62×10^{-13} $g^2cm^{-4}s^{-1}$ and 1.44×10^{-12} $g^2cm^{-4}s^{-1}$ for the GTBC, the two-layer TBC and the NiCoCrAlY coating, respectively. It is clear that the oxidation rates of both the GTBC and two-layered TBC are far below that of the NiCoCrAlY coating. The low oxidation rate of the two-layered TBC can be attributed to the increased protection of pre-oxides formed on the bond coat during pre-treatment in vacuum. On the other hand, the GTBCs have a better resistance to high-temperature oxidation than the two-layered TBCs, due to the formation of the dense Al_2O_3 layer on the bond coat during the preparation of the GTBC.

The change of the GTBC in microstructure was examined during testing. Fig. 3 shows an SEM micrograph and EDXS analysis of cross-section of the GTBC after 100 hr testing at 1323 K. The columnar microstructure of the YSZ topcoat remained basically the same as that before testing. However, there is a small increase of the Al_2O_3 layer in thickness. It is clear that outward diffusion of Al occurred during the testing by selective oxidation of the Al in the bond coat. In the meantime, it is found that an "inlaid" interface was formed between the Al_2O_3 layer and bond coat, which was caused by oxidation of the Al from the tablet of Al-Al_2O_3-YSZ that diffused into the gaps between the columns of the bond coat during the co-deposition of the tablet. It can be thought that the "inlaid" interface reinforced the adherence of Al_2O_3 layer to the bond coat. The analysis result of EDXS gives clear evidence that outward diffusion of Al occurred accompanying with the inward diffusion of oxygen into the bond coat during high-temperature oxidation. In addition, there was no sign of outward diffusion of Cr. This indicates that the Al_2O_3 layer can effectively prohibit the outward diffusion of Cr during high-temperature oxidation.

Fig. 4 compares XRD patterns (Cu K_α radiation) on the surface of the Al_2O_3-YSZ transition layer before testing and after 100 hr testing at 1323 K. The result of XRD analysis shows that the transition layer mainly consists of t-ZrO_2 phase and small amount α-Al_2O_3 phase. Some peaks from $\gamma + \gamma'$ phases are also detected, which are caused by the NiCoCrAlY bond coat. On the other hand, it is found that the relative intensity of $\gamma + \gamma'$ phase to that of ZrO_2 phase in the transition layer after 100 hr testing decreased as compared with that before testing. This confirms the above observation and analysis that the growth of Al_2O_3 layer is caused by oxidation of the bond coat.

3.3. High-temperature hot-corrosion tests

The tested specimens include the one coated with the traditional two-layered TBC and the other with the GTBC. Fig. 5 shows the weight changes of the tested specimens obtained during cyclic HTHC test. Compared with those tested in isothermal oxidation environment, the tested specimens showed a significant increase in weight before catastrophic failure. This means that the oxidation rates were greatly accelerated when the TBCs exposed to hot-corrosion environment. On the other hand, once deterioration started, the specimens showed abrupt loss in weight, suggesting that spallation of the coatings from the substrate occurred. The two-layered TBC failed after 180 hr of testing, whereas the

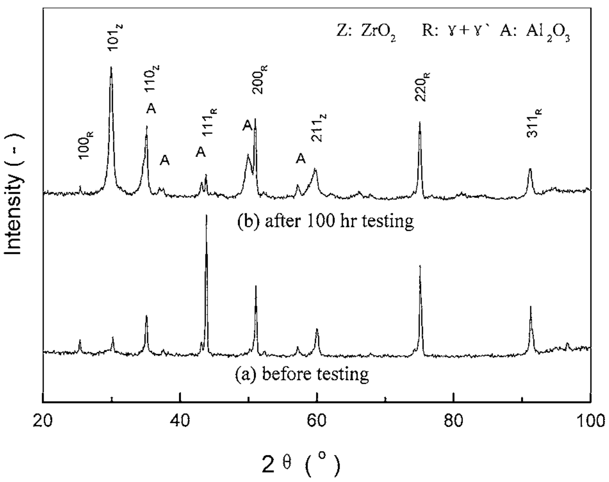

Figure 5 XRD patterns on the surface of the transition layer of the GTBC before testing (a) and after 100 hr testing in air at 1323 K (b).

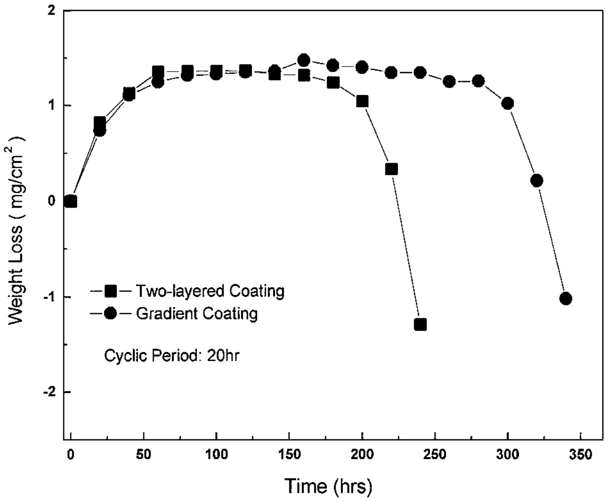

Figure 6 Plot of weight change vs. time for coated specimens during cyclic high-temperature hot-corrosion test in air at 1223 K.

GTBC improved the cyclic HTHC resistance by about 100 hr as compared with the two-layered TBC. This indicates the GTBC have a better resistance to cyclic HTHC attack than the traditional two-layered TBC.

The change in microstructure was examined during the cyclic HTHC test Fig. 6 shows SEM cross-sectional view of the GTBC after 300 hr testing. Compared with the one before testing, the YSZ topcoat shows no change in typical columnar grain microstructure and remains good adherence to the Al_2O_3-YSZ transition layer. However, catastrophic cracks developed in the surface layer of bond coat. It is clear that failure of the GTBC will take place by cracking at the interface between the bond coat/Al_2O_3 layer after few cyclic testing. The corresponding EDXS mappings, as shown in Fig. 7, indicate that O and S are enriched in the surface layer of bond coat. This means that S diffused into the bond coat during the fluxing of Al_2O_3 layer in Na_2SO_4. In the meantime, a certain concentration of Cr also presents in the surface layer besides its enrichment in the inner bond coat, suggesting outward migration of this element during the testing.

It is well known that there are large populations of pores between individual ceramic columns in the YSZ topcoat of both GTBCs and two-layered TBCs, which contribute to improve the tolerance of the TBCs to strain. Unfortunately, the deposits of fused Na_2SO_4 on the coatings can infiltrate into the bond coat through the pores in the YSZ topcoat during HTHC testing. The

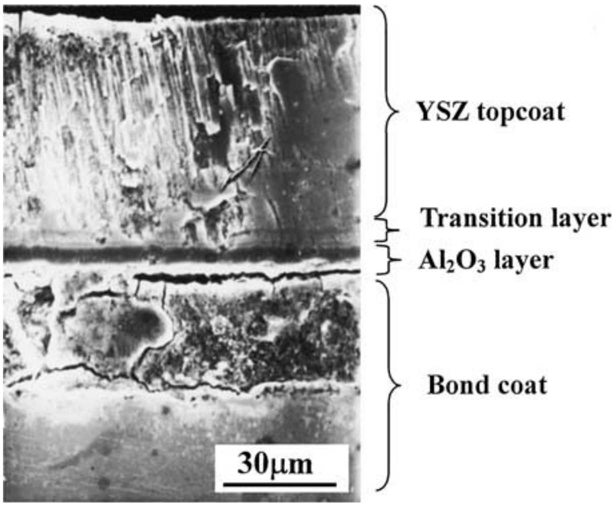

Figure 7 SEM cross-sectional view of the GTBC after 300 hr of cyclic high-temperature hot-corrosion test at 1223 K.

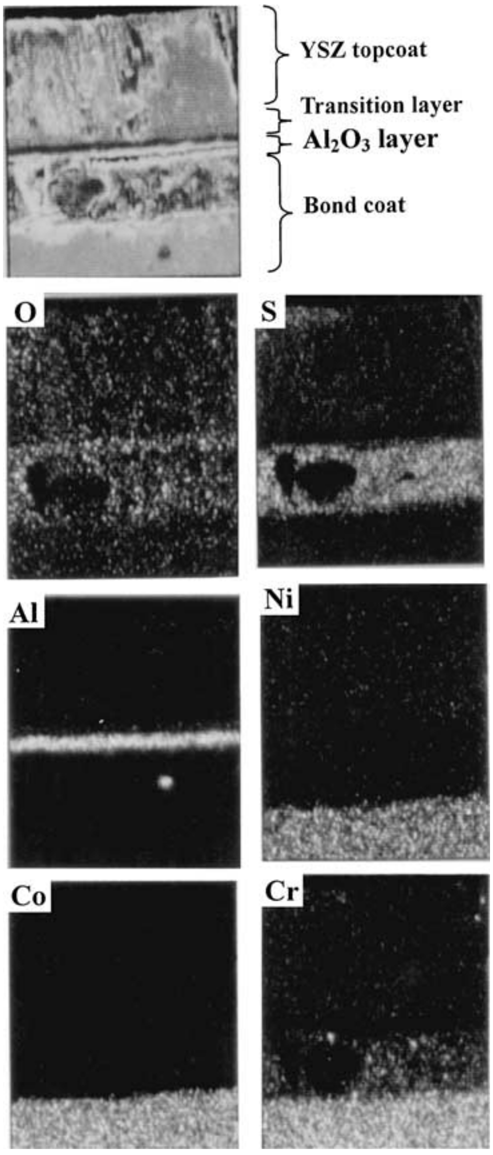

Figure 8 SEM cross-sectional view and EDXS analysis of the GTBC after 300 hr of cyclic high-temperature hot-corrosion test at 1223 K.

dense Al_2O_3 layer formed on the bond coat of GTBC effectively prohibits inward diffusion of oxidants such as O and S and outward diffusion of Al and Cr. It is possible that the initiation hot-corrosion stage of the GTBCs is significantly postponed as compared with that of the two-layered TBCs. In the meantime, the "inlaid" interface reinforced the adherence of Al_2O_3 layer to the bond coat. Additionally, thermal stresses were greatly relaxed in the GTBCs. Due to the above factors, the GTBCs revealed superior behavior of resistance to cyclic HTHC as compared with the two-layered TBCs.

The end of the initiation stage results from the penetration of Na_2SO_4 through the protective Al_2O_3 layer, due to fluxing of the protective oxides in Na_2SO_4 as acidic or basic solutes [19–22]. During propagation stage, the accelerated oxidation and sulfidation of the bond coat occurred. It is possible that the S reacts with the bond coat to form sulfides such as chromium sulfide in the surface layer of the bond coat as shown in Fig. 7. Cracks developed in the surface layer by the combined effect of the sulfides and thermal cycling, and finally led to failure of the GTBC.

4. Conclusions

Performance of the GTBCs was evaluated by isothermal oxidation and cyclic high-temperature hot-corrosion tests. Conclusions can be draw as follows:

1. The GTBCs exhibited better resistance to high-temperature oxidation and cyclic HTHC than traditional two-layered TBCs.
2. The dense Al_2O_3 layer formed on the bond coat can effectively prohibit inward diffusion of oxidants such as O and S and outward diffusion of Al and Cr.
3. An "inlaid" interface, the formation of which resulted from the oxidation of Al diffusion into the gaps between the columns of bond coat during the fabrication of the GTBCs, reinforced the adherence of Al_2O_3 layer to the bond coat.
4. S and O diffused into the bond coat during fluxing of the Al_2O_3 layer. Cracks developed in the surface layer of the bond coat by the combined effect of the sulfidation of bond coat and thermal cycling, and finally led to the failure of GTBCs by cracking at the interface between the bond coat and Al_2O_3 layer.

Acknowledgements

This research is sponsored by National Natural Science Foundation of China (NSFC) and Aviation Science Foundation of China (ASFC).

References

1. C. T. CANNISTRARO, *Adv. Mater. Process.* **139** (1991) 32.
2. I. E. SUMNER and D. L. RUCKLE, NASA Tech. Memo. TM-8112, 1980 (National Aeronautics and Space Administration).
3. R. E. DEMARAY, J. W. FAIRBANKS and D. H. BOONE, ASME Rep. 82-GT-264, 1982 (American Society of Mechanical Engineers, New York).
4. HUIBIN XU, SHENGKAI GONG and LIANG DENG, *Thin Solid Films* **334** (1998) 98.
5. XIAOFANG BI, HUIBIN XU and SHENGKAI GONG, *Surf. Coat. Technol.* **130** (2000) 122.
6. HUIBIN XU, HONGBO GUO, FUSHUN LIU and SHENGKAI GONG, *ibid.* **130** (2000) 133.
7. B. A. MOVCHAN and G. S. MARINSKI, *ibid.* **100/101** (1998) 309.
8. R. H. BARKALOW and F. S. PETTIT, in Proceedings of First Conference on Advanced Materials for Alternate-Fuel Capable Directly Fired Heat Engines ME (1979) p. 704.
9. R. L. JONES, S. R. JONES and C. E. WILLIAMS, *J. Electrochem. Soc.* **132** (1985) 1498.
10. A. S. JAMES, K. S. FANCEY and A. MATTHEWS, *Surf. Coat. Technol.* **32** (1987) 377.
11. J. T. PRATER and E. L. COURTRIGHT, *ibid.* **32** (1987) 390.
12. R. MÉVREL, *Mater. Sci. Eng.* A **120** (1989) 13.
13. K. Y. KIM, S. H. KIM, K. W. KWON and L. H. KIM, *Oxidation of Metals* **41** (1994) 179.
14. K. Y. KIM, J. H. JUN and H. G. JUNG, *ibid.* **40** (1993) 321.
15. D. R. MUMM and A. G. EVANS, *Acta. Mater.* **48** (2000) 1815.
16. D. R. CLARKE, R. J. CHRISTENSEN and V. TOLPYGO, *Surf. Coat. Technol.* **94/95** (1997) 89.
17. Z. A. CHAUDHURY, G. M. NEWAZ, S. Q. NUSIER and T. AHMED, *Mater. Sci. Eng.* A **231** (1997) 34.
18. F. H. STOTT and G. C. WOOD, *Corrosion Science* **3** (1971) 79.
19. J. A. GOEBEL and F. S. PETTIT, *Metall. Trans.* **2** (1973) 2875.
20. J. A. GOEBEL, F. S. PETTIT and G. W. GOWARD, *ibid.* **4** (1973) 261.
21. R. A. RAPP, *Mater. Sci. Eng.* **87** (1987) 319.
22. Y. LONGA-NAVA, Y. S. ZHANG, M. TAKEMOTO and R. A. RAPP, *Corrosion Science* **52** (1996) 680.

Received 10 April
and accepted 17 December 2001